

Southern Africa Validation of the MODIS, L3JRC, and GlobCarbon Burned-Area Products

David P. Roy and Luigi Boschetti

Abstract—Three available global multi-annual burned area products (L3JRC, GlobCarbon, and MODIS) are validated for a burning season across southern Africa. Validation is undertaken using the same independent reference data and using the same validation and reporting protocol. The independent reference data were derived by interpreting multitemporal Landsat Enhanced Thematic Mapper Plus data to map the location and approximate date of burning at 11 Landsat scenes distributed across southern Africa and covering approximately 295 000 km². The accuracy of the products was quantified using metrics derived from confusion matrices to characterize product accuracy for local applications and using metrics derived through a linear regression on a 5 × 5 km grid to characterize product accuracy for coarser scale applications. Quantitative results are described, and the differences between the products are discussed.

Index Terms—Burned area, satellite, validation.

I. INTRODUCTION

THE POTENTIAL research, policy, and management applications of satellite products place a high priority on providing statements about their accuracy [38]. Intercomparison of products made with different satellite data and/or algorithms provides an indication of gross differences and, possibly, insights into the reasons for the differences; however, product comparison with independent reference data is needed to determine accuracy [25]. Validation is the term used here and, more generally, to refer to the process of assessing satellite product accuracy by comparison with independent reference data. Validation is required to provide accuracy information to help users decide if and perhaps how to use a product and, combined with product quality assessment [48], to identify needed product improvements [36], [61].

The need for a validated long-term record of global burned area was initially established in the context of the international global observing system [20] and was refined by the Committee on Earth Observation Satellites (CEOS) and the Global Climate Observing System to meet the needs of the U.N. Framework

Convention on Climate Change [74]. There are several outstanding issues in the development of a global-scale burned-area product validation methodology. These include the need to increase the quality and economy of validation by developing and promoting an international network of validation sites and by establishing accuracy assessment and reporting protocols [25], [36], [38], [68]. Common validation sites afford opportunities for independent reference data sharing and can be expected, with the development of validation protocols, to foster standardization of product accuracy reporting. These needs have long been advocated by fire product producers and product users, for example, at the International Geosphere–Biosphere Program Data and Information Services working group meeting on remote sensing of fires, held in Toulouse, France, on March 19–20, 1998, and at the joint Global Observation of Forest Cover (GOFC)/CEOS Land Product Validation Fire Satellite Product Validation Workshop, held in Lisbon, Portugal, on July 9–11, 2001 [46]. Despite the number of publicly available global-satellite-derived burned-area products, including the Global Burned Area 2000 (GBA2000) [21], [65], GLOBSCAR [57], GlobCarbon [44], Leicester, Louvain-la-Neuve, Lisbon, and JRC (L3JRC) [66], and the Moderate Resolution Imaging Spectroradiometer (MODIS) [50], [53] products, there has been neither rigorous assessment of their accuracy nor development of systematic assessment methodologies. Arguably, this has been because of limited resources and because of the scope and complexity of the task. Limited product comparison studies have revealed large discrepancies in the areal estimates, timing, and location among satellite fire products and highlight the need for systematic product validation (e.g., [5] and [30]).

The validation of satellite active fire products is difficult because of practical problems in collecting independent reference data that characterize the location and physical properties of actively burning fires. Previous approaches have used independent reference data from aircraft observations of prescribed fires and wildfires (e.g., [29]). Aircraft campaigns are expensive to undertake in a regionally or globally representative manner and are difficult to coordinate with cloud-free conditions at the time of satellite overpass. Similarly, although ground-based fire measurements may provide useful information, they are difficult to coordinate over large areas [9]. Burned areas mapped from high spatial resolution satellite data may be used to validate active fire products but do not provide a reliable validation if the high spatial resolution data were sensed when the fires were inactive or cloud covered and may not provide information on active fire product commission errors [22], [43]. High spatial resolution ASTER data have been used to validate the MODIS Terra active

Manuscript received June 11, 2008; revised September 15, 2008. Current version published March 27, 2009. This work was supported in part by the NASA Earth System Science Program under Grant NNG04HZ18C and in part by the NASA Land-Cover and Land-Use Change (LCLUC) Program under Grant NAG511251.

D. P. Roy is with the Geographic Information Science Center of Excellence, South Dakota State University, Brookings, SD 57007 USA (e-mail: david.roy@sdstate.edu).

L. Boschetti is with the Department of Geography, University of Maryland, College Park, MD 20742 USA (e-mail: luigi.boschetti@hermes.geog.umd.edu).

Digital Object Identifier 10.1109/TGRS.2008.2009000

fire product, as both data are collected simultaneously from the same satellite which largely overcomes these timing and synoptic coverage issues [11], [37].

The validation of burned-area products generated by direct mapping from reflective wavelength satellite data does not require the simultaneous collection of independent reference data with satellite overpasses. This is because the surface effects of fire are persistent, with a persistence observed in satellite data varying from weeks (grassland ecosystems) to years (typically forest ecosystems) [41], [67]. Consequently, independent reference data derived from high spatial resolution satellite data, such as Landsat, have been used to validate lower spatial resolution burned-area products (e.g., [3], [7], [17], [59], [60], and [66]).

In this paper, the three most recent global multiannual burned-area products generated at satellite native resolution are validated for the 2001 burning season across southern Africa, specifically the L3JRC [66], GlobCarbon [44], and MODIS [50] burned-area products. A regional validation is undertaken using the same independent reference data derived from multitemporal Landsat data and using the same validation and reporting methodology.

II. GLOBAL BURNED-AREA PRODUCTS

A. L3JRC Burned-Area Product

The L3JRC burned-area product [66] was developed as a collaboration between the University of Leicester, U.K., the Université Catholique de Louvain, Belgium, the Instituto de Investigação Científica Tropical, Portugal, and the Joint Research Centre of the European Commission, Italy. It is a multiannual burned-area product which builds on the heritage of the GBA2000 product [65]. Like GBA2000, the L3JRC product is generated from 1-km SPOT-VEGETATION data, but instead of using regionally specific algorithms, it implements globally a refined version of the boreal Eurasia GBA2000 algorithm developed by the International Forest Institute (IFI) [14]. The L3JRC algorithm uses a change detection approach. After preprocessing to remove clouds and shadows, a reference composite image is created, moving forward in time in daily steps, with each step keeping the most recent noncontaminated observation. At each step, an index based on the near-infrared reflectance (NIR) is computed, comparing the new observation with the previous composite, and the mean and standard deviation of the index computed over a 200-km \times 200-km window. A pixel is flagged as burned if its index value is lower than the mean minus two times the standard deviation, and using spectral tests based on the 0.83- and 1.66- μm reflective bands. Postprocessing using land cover information from the GLC2000 vegetation map [35] is applied to reduce commission errors [66].

The L3JRC product is available as an annual 1-km product, as a global binary raster file in the Plate Carrée projection. Each L3JRC pixel defines the Julian day of the first burned area detection within a fire year starting on the 1st of April (if a pixel burns more than once per year, only the first day of burning is stored), or a zero value to indicate that no

burning was detected [66]. L3JRC product validation was conducted comparing the proportion of area burned from L3JRC with proportions derived from 72 globally distributed Landsat scenes, using 3000-km² hexagonal cells. The coarse resolution of the cells makes this assessment only moderately spatially specific; [66] reported that for Africa and the Middle East, the L3JRC product mapped approximately 54% of the area burned.

B. GlobCarbon Burned-Area Product

The GlobCarbon project, promoted by the European Space Agency, has generated a number of land products, including a global monthly 1-km burned-area product, for assimilation into global carbon models [44], [75]. The GlobCarbon burned-area product is generated using two regional GBA2000 algorithms and the GLOBSCAR algorithms [57] applied to 1-km SPOT-VEGETATION and ERS2-ATSR2/ENVISAT AATSR data, respectively. The two GBA2000 algorithms are the IFI algorithm (the same used by the L3JRC product, independently implemented) and the Technical University of Lisbon (UTL) algorithm developed for southern Africa [58]. The UTL algorithm uses a change detection approach, where daily observations are compared against a monthly minimum-NIR composite. A pixel is defined as burned by applying a fixed set of spectral thresholds (defined *a priori* by linear discriminant training analysis) to observed reflectance and the change between the observed and composited NIR reflectance. The GLOBSCAR algorithm, applied to ERS2-ATSR2 for 1998–2002 and to ENVISAT AATSR data for 2003–2007, is based on two separate algorithms. The K1 GLOBSCAR algorithm uses the NIR and thermal infrared (TIR) bands with an adaptive contextual window-based approach that assumes that burned vegetation has lower NIR reflectance and higher daytime TIR brightness temperature than surrounding unburned vegetation [40]. The E1 GLOBSCAR algorithm is based on five fixed thresholds applied to red, shortwave infrared, NIR, and TIR brightness temperature values [15]. A pixel is considered as burned by GLOBSCAR if it is flagged as such by both the K1 and E1 algorithms and if it does not fall within certain nonburnable areas including deserts and water bodies [57].

The GlobCarbon product is available as a monthly 1-km product, as a global binary raster in the Plate Carrée projection. Each GlobCarbon pixel defines the Julian day of the first burned-area detection within the month, and which algorithm(s) detected it, or a zero value to indicate that no burning was detected.

C. MODIS Burned-Area Product

The NASA MODIS on the Terra and Aqua satellites has specific features for fire monitoring [26], [29]. A bidirectional-reflectance-model-based change detection approach is applied independently to each gridded MODIS pixel to take advantage of the spectral, temporal, and structural changes that characterize vegetation fire [50]. MODIS reflectances sensed within a temporal window of a fixed number of days are used to predict the reflectance on a subsequent day. Rather than

attempting to minimize the directional information present in wide field-of-view satellite data by compositing, or by the use of spectral indices, this information is used to model the directional dependence of reflectance, commonly defined by the bidirectional reflectance distribution function (BRDF). This provides a semiphysically based method to predict change in reflectance from the previous state. A statistical measure is used to determine if the difference between the observed reflectance and the BRDF model predicted reflectance in the near and middle infrared bands indicates a significant change of interest. This approach is repeated independently for each pixel, moving through the reflectance time series in daily steps. A temporal constraint is used to differentiate between temporary changes, such as shadows, which are spectrally similar to more persistent fire-induced changes. The identification of the date of burning is constrained by the frequency and occurrence of missing observations, and to reflect this, the algorithm is run to report the burn date with an eight-day precision.

The MODIS burned-area product is available as a monthly gridded 500-m product defined, like the other Collection 5 geolocated MODIS land products, in the sinusoidal equal-area projection in fixed earth-location tiles, each covering approximately 1200×1200 km ($10^\circ \times 10^\circ$ at the equator) [72]. Burning detected in the middle month plus and minus eight days (the detection precision) is reported. For each gridded land pixel, information, including the following, is described: the approximate Julian day of burning, or a code indicating unburned, or no burning detected but snow detected, or no burning detected but water detected, or insufficient number of MODIS observations to make a detection decision (usually due to cloud or missing data), and ancillary processing path and quality information.

III. STUDY AREA AND INDEPENDENT REFERENCE DATA

A. Southern Africa Biomass Burning

Fire is prevalent throughout southern Africa, with a prolonged annual dry season combined with relatively rapid rates of fuel accumulation that create conditions conducive to frequent vegetation fires [70]. Africa has, by continent, the most extensive burning globally [13], [65], [71]. In southern Africa, most fires occur in the dry season, particularly July to September, when herbaceous vegetation is either dead (annual grasslands) or dormant, and when deciduous trees have shed their leaves, thereby contributing to an accumulation of dry and fine fuels that are easily combustible [55]. The occurrence and spatial distribution of fire is a function of contrasting physical influences acting under different circumstances at different scales [4], [16]. The fraction of the landscape that burns across the region varies greatly because the propensity to burn is influenced by weather conditions, the presence of ignition sources, and the amount, type, and arrangement of the available fuel, all of which change across space and through time and are mediated by climatic and anthropogenic factors [1]. In wet regions, above about 1000–1200-mm rain per year, where there is sufficient rainfall to support closed-canopy woodlands and forests, prolonged moist conditions and heterogeneous

TABLE I
LANDSAT ETM+ ACQUISITIONS USED TO PRODUCE
VALIDATION DATA SETS

Country Landsat Path/Row	Landsat acquisition dates 2001	Landsat area mapped between acquisition dates
Mozambique 165/070	14th September - 30th September	28263 km ²
South Africa 168/078	18th August - 3rd September	502 km ²
South Africa 168/077	18th August - 3rd September	28614 km ²
Malawi 169/069	25th August - 26th September	828 km ²
Zimbabwe 169/074	10th September - 12th October	4116 km ²
Zimbabwe 171/073	23rd August - 24th September	33333 km ²
Zimbabwe 172/073	14th August - 1st October	33082 km ²
Botswana 174/074	29th September - 15th October	33735 km ²
Botswana 175/073	19th August - 4th September	33383 km ²
	4th September - 6th October	33258 km ²
Namibia 179/073	15th August - 2nd October	32982 km ²
Namibia 180/073	6th August - 23rd September	32053 km ²

vegetation structure constrain the spread of fires even if the fuel load is high [70]. Fires are larger and more contiguous in the grasslands and open savanna woodlands at intermediate rainfall amounts (about 550–750 mm per year) where there is sufficient grass production to produce hot fires that can damage trees, but not enough rainfall to allow their rapid regeneration and closure of their canopies, which would otherwise restrict grass production [56]. The majority of fires are thought to be anthropogenic, lit for numerous reasons, but the influence of humans, for example, in altering fuel loads and structure and increasing or suppressing fire is poorly understood at regional scale [1], [19].

B. Independent Reference Data

The independent reference data used in this paper were collected as part of the Southern Africa Regional Science Initiative (SAFARI 2000) intensive dry season campaigns that were timed to coincide with the peak southern African biomass burning months [64]. SAFARI 2000 provided an early opportunity to use and regionally validate the MODIS satellite products [45]. Independent reference data were derived from Landsat Enhanced Thematic Mapper plus (ETM+) satellite data. Eleven Landsat scenes, each covering approximately 180×170 km defined in the UTM coordinate system and referenced by a unique Landsat Worldwide Reference System (WRS-2) path and row coordinate [2], were selected (Table I). The 11 scenes together cover approximately 3% of the surface of southern Africa and were distributed geographically to encompass representative subcontinental variation in burned-area characteristics and where members of the southern Africa Fire Network (SAFNet) were working [51]. Some of the scenes were quite remote and inaccessible, for example, the Mozambique scene, which had restricted road access and land mines.

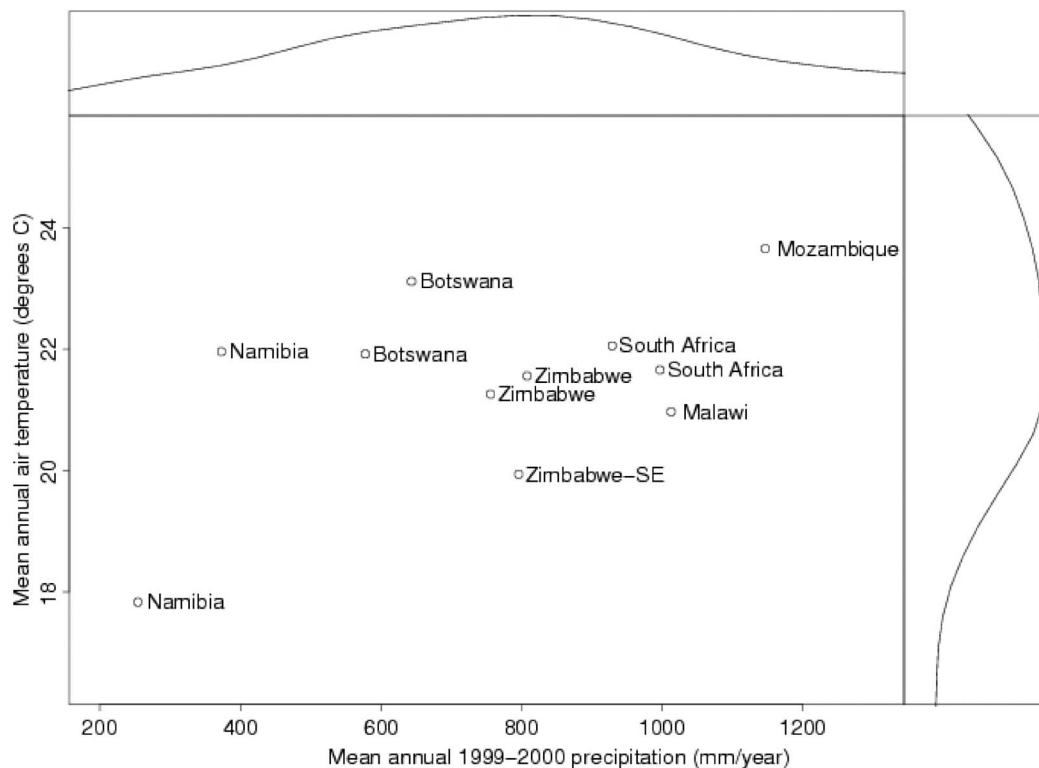


Fig. 1. Mean annual air temperature (derived from 0.5° mean monthly 2-m air temperature climatology data; [33]) plotted against mean 1999 and 2000 annual precipitation (derived from the monthly Tropical Rainfall Measuring Mission best estimate precipitation rate product; [23]) at the geographic centers of the 11 Landsat ETM+ scenes (Table I). Probability densities of the mean annual temperature and mean 1999 and 2000 annual precipitation for all of southern Africa (including Madagascar) are shown in the plot margins. This figure is adapted from [51].

Fig. 1 is taken from [51] and shows the 11 Landsat scenes in “meteorological space,” showing their mean 1999 and 2000 annual precipitation amounts and mean annual air temperature. The Fig. 1 margins show probability densities of the mean annual temperature and mean 1999 and 2000 annual precipitation for all of southern Africa—indicating that the scenes encompass a wide range of the regional variation of these variables. The scenes are geographically distributed approximately west to east from hot arid savanna (Namibia) to hotter moister woodland (Mozambique). This distribution corresponds approximately to increasing plant water availability, which is a regionally controlling factor on the type and amount of vegetation, and so indirectly on human population density and land use, which together influence the frequency, timing, size, and spatial distribution of burned areas. The characteristics and land-cover–land-use practices at the scenes are described in detail in [51].

In this paper, Landsat data acquired in 2001 were used, as all three global burned-area products were reliably generated in 2001. The MODIS burned-area product was temporally incomplete in 2000, as the input MODIS data quality was poor prior to September 2000 [48] and the GlobCarbon product had projection problems in the Southern Hemisphere in 2002 (Steven Plummer, personal communication, February 2008).

The Landsat data were interpreted to derive high spatial resolution maps of the location and approximate date of burning. At least two Landsat ETM+ data acquisitions were obtained per scene, as using only one acquisition precludes the ability to determine when a burn occurred, i.e., in pre-

vious months or years, and interpreting two acquisitions together helped improve the interpretation [51]. A primary problem in obtaining multitemporal Landsat data outside of the United States is in ensuring that the data are acquired [24]. To specifically support the needs of SAFARI 2000, and the MODIS burned-area product validation, the 11 scenes were designated a priority acquisition status by the U.S. Landsat project, guaranteeing their acquisition during the dry season [45], [51]. From these, consecutive ETM+ acquisitions (16 days apart) spanning significant biomass burning events under relatively cloud-free conditions were selected whenever possible.

The interpretation at each Landsat scene was undertaken by members of SAFNet. SAFNet is a contributing network to the GOF/Global Observation of Landcover Dynamics-Fire initiative which has a guiding principle that the user community plays an active role in defining satellite fire-product requirements and in undertaking product assessment [12], [28]. SAFNet members were able to undertake limited fieldwork as part of their existing scientific, resource management, and environmental assessment activities and had expert knowledge of the local drivers of biomass burning. A consensus interpretation protocol was developed to ensure compatibility of the independent reference data derived by different SAFNet members and to allow the data to be scaled up to provide meaningful subcontinental validation data. The interpretation approach is described in [51] and was based upon multitemporal visual comparison of the ETM+ near- and middle-infrared bands, augmented by the ETM+ thermal band and a spectral index

that is sensitive to burned vegetation, to define the boundaries of the following:

- 1) the mapped region, i.e., falling within the geographic union of the two ETM+ acquisitions;
- 2) areas within the mapped region that could not be interpreted, e.g., because of cloud occurring in one or more ETM+ acquisitions, or inaccessible areas that could not be unambiguously interpreted;
- 3) burned areas interpreted as having occurred between the two ETM+ acquisition dates.

In this way, parts of the Landsat scenes that could not be interpreted, or that could not be mapped, would not be mistakenly considered unburned when the Landsat independent reference data were compared with the global burned-area products.

To reduce the mapping effort, particularly in scenes containing large numbers of small and spatially fragmented burns, a minimum mapping unit of 240 m was adopted, whereby only burned areas with small axis dimensions of 240 m or greater were mapped. This dimension was selected, as it is an integer multiple of the ETM+ 30-m reflective and 60-m thermal-band pixel dimensions [51].

IV. DATA PROCESSING

The three global burned-area products have different spatial and temporal resolutions and formats. Some processing, described hereinafter, was undertaken to produce comparable burned-area data sets encompassing the temporal interval covered by the Landsat independent reference data and to coregister the data.

The GlobCarbon product is distributed as a monthly 1-km product. The monthly products encompassing the first and the second Landsat acquisition dates at each scene (Table I) were temporally composited into a single 1-km raster image; any pixels labeled as burned by GlobCarbon between or on the Landsat acquisition dates were considered as burned, and all other pixels falling within the Landsat scene were considered unburned. In this paper, if any of the GlobCarbon algorithms detected a burned pixel, it was considered as burned.

The L3JRC product is available as an annual 1-km product. Each L3JRC pixel defines the Julian day of the first burned-area detection within a fire year starting on the first of April, which is before the earliest Landsat acquisition date (Table I). As with the GlobCarbon product, any L3JRC pixels labeled as burned between or on the Landsat acquisition dates were considered as burned, and all other pixels falling within the scene were considered unburned.

The MODIS burned-area product is available as a monthly 500-m product reporting the approximate day of burning, between eight days before and after the calendar month period. Consequently, there is always a 16-day overlap period between consecutive months in which the same burn can be detected on the same day or, because of algorithm sensitivity to the frequency and occurrence of missing observations, on slightly different days. For this study, a temporally filtered version of the monthly product that uses the product quality and

processing path information to allocate burns in the overlap period to the most likely calendar month was used in order to preclude potential double counting of burned areas when consecutive months are considered. These temporally filtered monthly products were temporally composited to encompass the first and second Landsat acquisition dates at each scene; any 500-m pixels labeled as burned between or on the Landsat acquisition dates were considered as burned, pixels labeled as unburned were considered unburned, and pixels labeled as no burning detected but water detected, or insufficient number of observations to make a detection decision (usually due to cloud or missing data), were considered as missing.

Considerable effort was taken to ensure that these temporally composited burned area data products were precisely coregistered with the Landsat independent reference data. The MODIS geolocation error is approximately 50 m at nadir [73], SPOT geolocation accuracy is approximately 300 m [76], and information on ERS2-ATSR2 geolocation accuracy is not publicly available but is assumed to be less than the 1-km pixel dimension. The Landsat L1G geolocation error is less than 250 m (1σ) and may be comparable to the MODIS error in areas of flat relief [32], [54]. The three temporally composited global burned-area data products were reprojected into registration with the Landsat UTM projection of each scene. Nearest neighbor resampling was used to maintain the pixel values; output pixel dimensions were set to 30 m to reduce nearest neighbor resampling pixel shifts (i.e., position errors) and to allow for direct comparison with the 30 m Landsat independent reference data.

V. VALIDATION METHODOLOGY

Moderate-resolution burned-area products have multiple users, who are interested in knowing the accuracy of different aspects of the product, and consequently, there can be no single accuracy measure synthesizing the information needs of all [7], [52], [68]. Generally, users are interested in the per-pixel detection accuracy for local-scale applications, e.g., for ecological and resource management applications, and users are interested in the precision and accuracy of total burned-area estimates at scales much coarser than the pixel size for large-area reporting purposes and applications such as fire emission modeling. Here, we use engineering conventions where precision indicates the repeatability of a set of measurements, usually expressed in terms of their standard deviation, and accuracy is the freedom from mistakes or error of the measurements, i.e., their conformity to independent reference data.

A. Local Product Accuracy

The accuracy of burned-area product detection at local scale can be effectively characterized through the confusion matrix and the accuracy indices derived from it [10], [18], [63]. Two-way burned/unburned confusion matrices were generated for each Landsat scene by comparison of the reprojected 30-m global burned-area products with the corresponding 30-m Landsat pixels, only considering the interpreted land within the Landsat-mapped region (Section III-B) and only considering

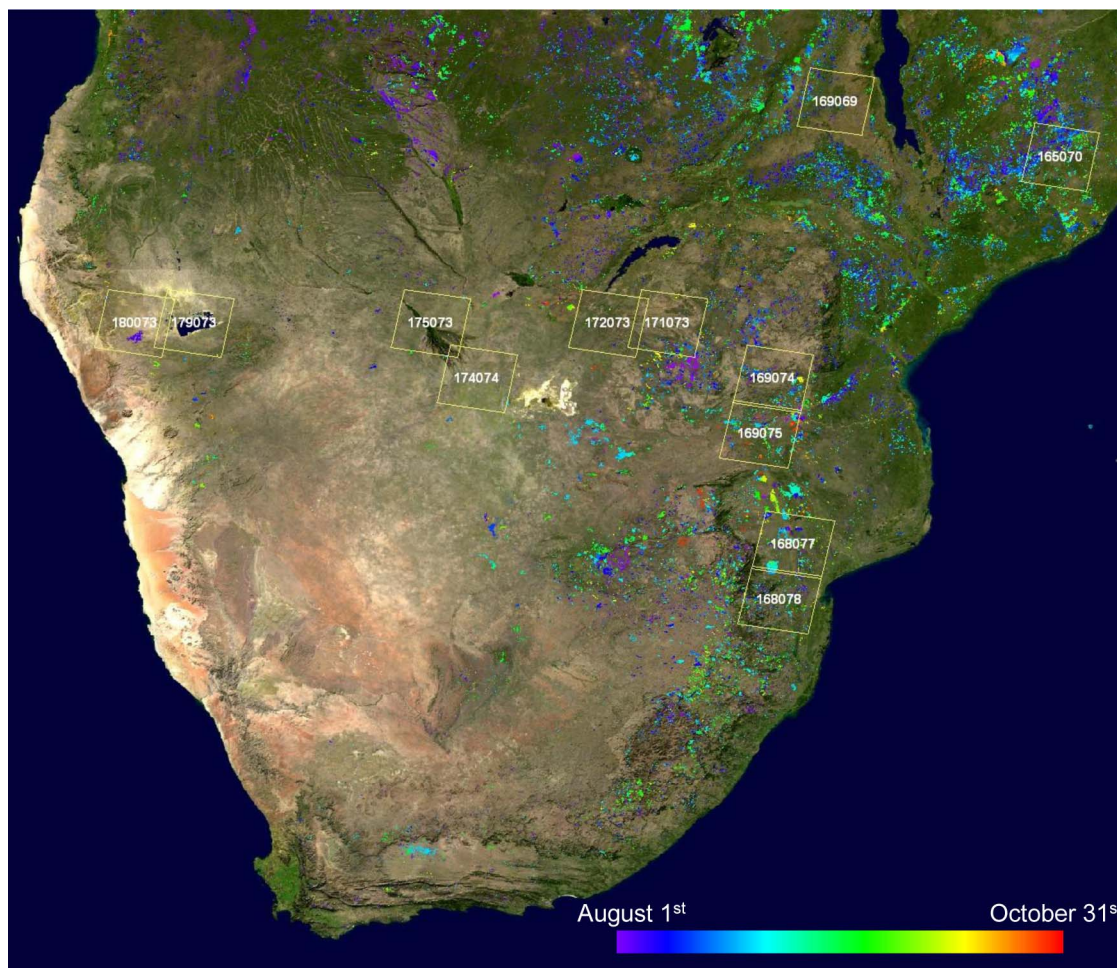


Fig. 2. L3JRC burned-area product displayed in a rainbow color scale according to the detection date, from blue (August 1, 2001) to red (October 31, 2001). To provide geographic context, the burned areas are superimposed on the NASA Blue Marble true-color MODIS surface reflectance composite. The boundaries of the 11 Landsat ETM+ validation scenes (Table I) are shown as yellow vectors.

30-m reprojected global burned-area products that were labeled as burned or unburned.

The percentage of correct pixels (i.e., both burned pixels and unburned pixels correctly classified), the commission error (i.e., the probability that a pixel mapped as burned in the moderate-resolution product is not burned in the reference data), and the omission error (i.e., the probability that a pixel mapped as burned in the reference data is not mapped as burned in the moderate-resolution product) were derived from the confusion matrices for each of the 11 Landsat scenes.

B. Regional Product Accuracy and Precision

An estimate of the accuracy and precision of the detection at subcontinental scale was inferred by comparing through a linear regression [7], [15], [59] the proportions of grid cells labeled as burned by the global burned-area product plotted against the proportions labeled as burned by the Landsat interpretation, considering together the data from all 11 Landsat scenes. Only the interpreted land within the Landsat-mapped region and only the 30-m reprojected global burned-area products that were labeled as burned or unburned were considered. In addition, only grid cells with less than 10% missing data were considered; the GlobCarbon and L3JRC burned-area products have no missing

data class, so this 10% threshold only affected the MODIS product analysis.

Geographical analyses of this kind are sensitive to the size and location of the grid cells; using increasing larger grid cell sizes will inflate statistical measures of correlation between the products [39], [69]. Consequently, a small 5-km grid cell dimension was selected, as it is larger than the coarsest 1-km global burned-area product pixel size, and significantly larger than the geolocation errors in the three global burned-area products, while being sufficiently small to reduce the occurrence of cells with similar burned-area proportions in both the burned-area product and Landsat data but with burns mapped at different locations within the cell.

VI. RESULTS

A. Local Product Accuracy

Figs. 2–4 show the areas detected as burned by the three global burned-area products during the dry season period, August to October 2001, which encompasses the Landsat acquisition dates (Table I). The burned areas are illustrated with a rainbow color scale to show the day of detection and are superimposed on a true-color MODIS surface reflectance

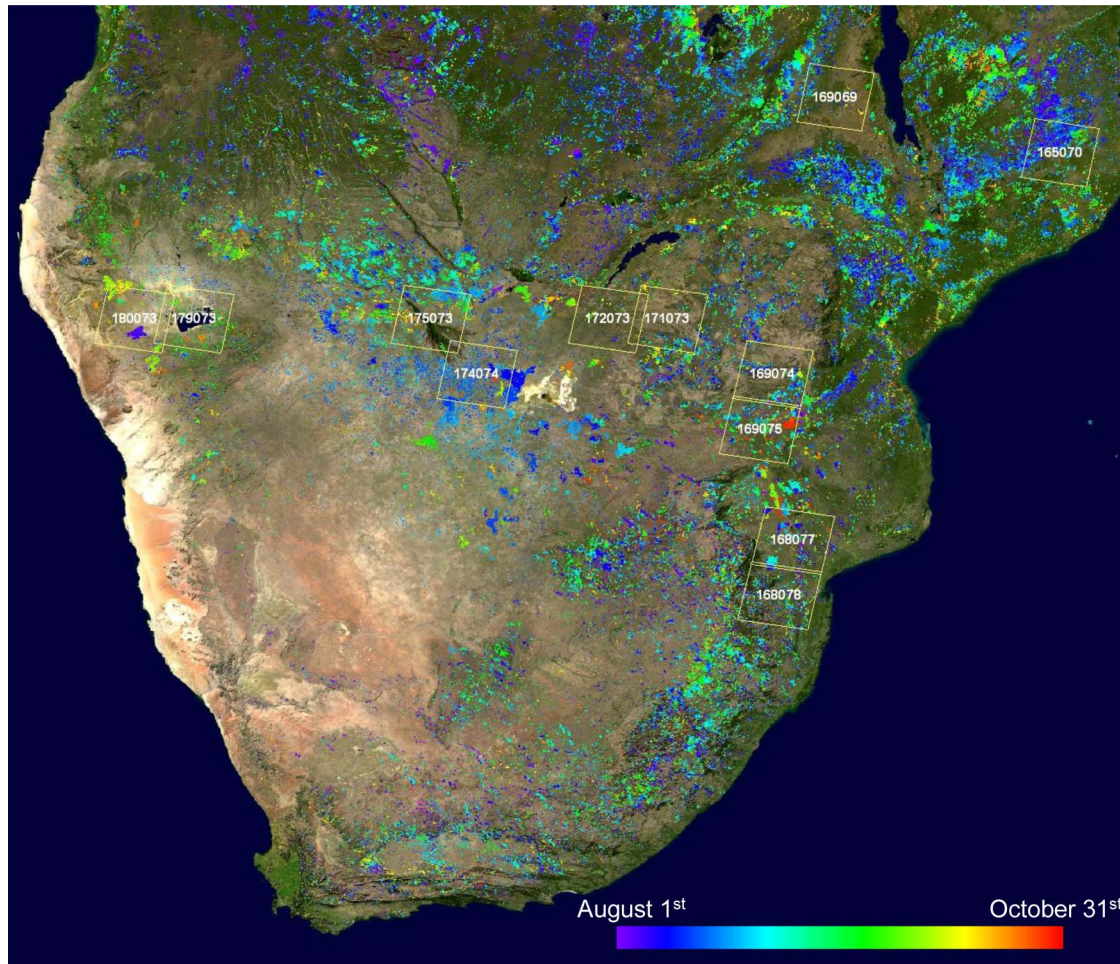


Fig. 3. GlobCarbon burned-area product displayed in a rainbow color scale according to the detection date, from blue (August 1, 2001) to red (October 31, 2001). To provide geographic context, the burned areas are superimposed on the NASA Blue Marble true-color MODIS surface reflectance composite. The boundaries of the 11 Landsat ETM+ validation scenes (Table I) are shown as yellow vectors.

composite to provide geographic context. The boundaries of the 11 Landsat scenes are shown as yellow vectors and are clearly distributed across a range of vegetation (specifically arid grassland in the west to Miombo woodland in the east). Qualitative visual inspection indicates significant differences in the area and the spatial distribution of burning among the three global burned-area products.

Tables II–IV summarize, for each Landsat scene, the accuracy of the L3JRC, GlobCarbon, and MODIS products. The percentages of the mapped areas reported as burned by the Landsat interpretation and by the burned-area product are shown in the second and third columns of these tables. The Landsat interpretations reported a greater percentage area burned than the corresponding burned-area product for all L3JRC scenes (Table II), for all MODIS scenes except for a single Namibian scene (Table IV), and for all but four GlobCarbon scenes (Table III). This is not unexpected, as the Landsat scenes encompass only a relatively small proportion of burned areas, ranging from 1.8% to 11.0% (Tables II–IV), and, except for parts of the Botswanan and Namibian scenes, include burned areas that are small and/or spatially fragmented relative to the spatial resolutions of the three global burned-area products [51]. It is well established that burned areas that are small and/or spatially fragmented relative to satellite

observations may not be detected reliably [15], [31], [49], [59]. Furthermore, the majority of fires in southern Africa are thought to be ground fires, and so, obscuration by overstory vegetation in regions with high leaf area index and percent tree cover may have also occurred [42], [53].

The percent correctly classified values in Tables II–IV are broadly similar among the three products, with lowest percent correct values among the 11 scenes of 88.9% (L3JRC), 88.6% (GlobCarbon), and 91.0% (MODIS). The percent correct statistic is not a particularly diagnostic measure for dichotomic classifications, particularly when the class of interest covers a small portion of the scene [6], as in this paper. The commission and omission errors reveal more information and greater differences among the products. To aid interpretation, commission and omission errors greater than 0.5 are reported in bold in Tables II–IV. Generally, burned-area product producers seek to reduce errors of commission at a cost of inflating omission errors; this is perhaps because certain product users do not wish to waste resources on visiting burned areas that did not actually occur [68] and perhaps because commission errors are more easily identified as part of product quality assessment and algorithm tuning procedures. Regardless of the reasons, this pattern is observed in the results, with generally lower errors of commission than omission. Six of the Landsat scenes have

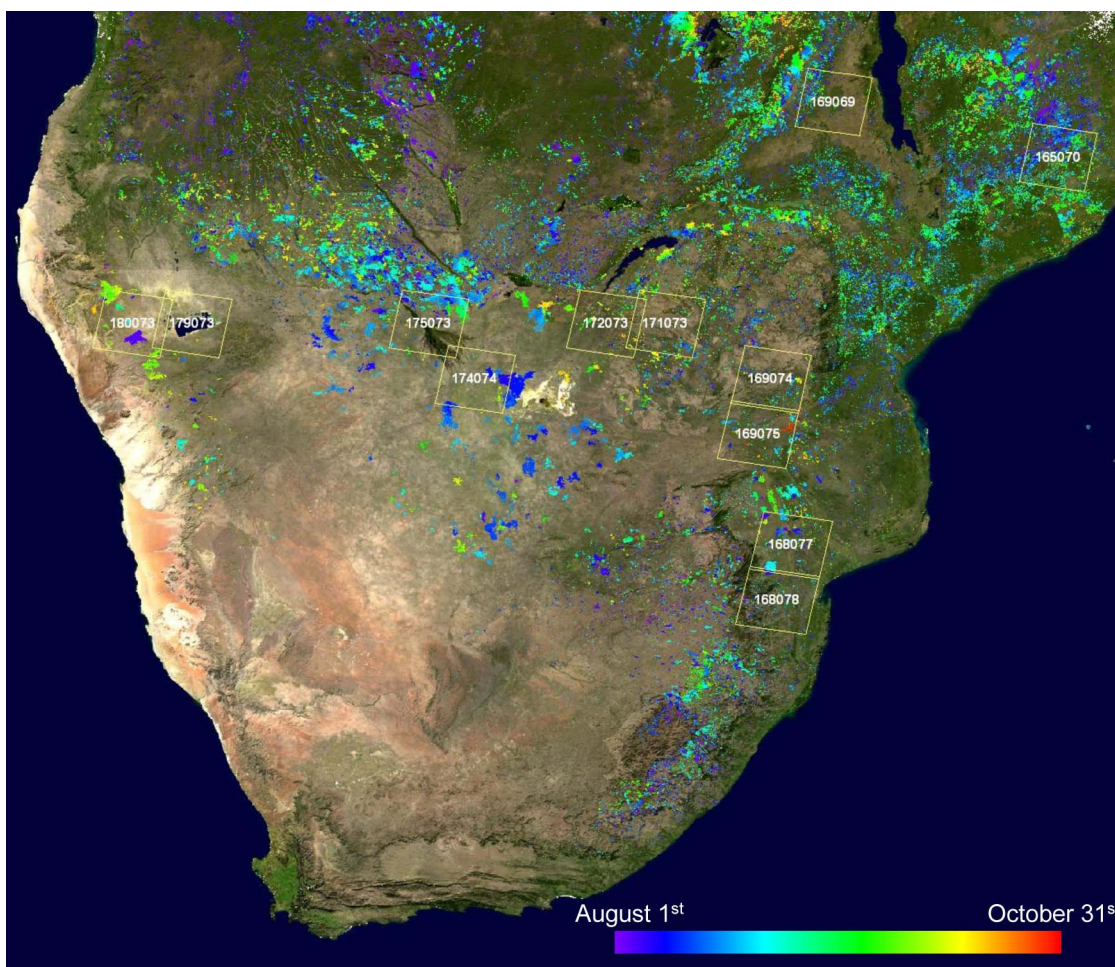


Fig. 4. MODIS burned-area product displayed in a rainbow color scale according to the detection date, from blue (August 1, 2001) to red (October 31, 2001). To provide geographic context, the burned areas are superimposed on the NASA Blue Marble true-color MODIS surface reflectance composite. The boundaries of the 11 Landsat ETM+ validation scenes (Table I) are shown as yellow vectors.

a L3JRC commission error greater than 0.5, five scenes have a GlobCarbon commission error greater than 0.5, and four scenes have a MODIS commission error greater than 0.5. Eight scenes have GlobCarbon and MODIS omission errors greater than 0.5, and all 11 Landsat scenes have a L3JRC omission error greater than 0.5; evidently, at subcontinental scale, the L3JRC product is relatively under detecting the area burned.

There is considerable variation in the commission and omission errors between scenes and products. Some caution must be taken in comparing scene results, as the SAFNet-interpreted areas varied; in particular, less than about 15% of each Landsat scene was interpreted for scenes in South Africa (168/078), Malawi (169/069), and Zimbabwe (169/074) (Table I). One Namibian scene (179/073) was rather unreliably mapped by the global burned-area products, particularly by the L3JRC product, even though the burns were spatially extensive. This may have been due to the arid nature of the site and the relatively low spectral change in reflectance due to fire. The Malawi scene (169/069) also had high errors, which may be related to the small and fragmented nature of the burned areas there, although only a small Landsat area was mapped (Table I). Full investigation of the reasons for the product and scene differences is beyond the scope of this paper and, for example, is also related to remote sensing factors including the algorithms,

and the amount and quality of satellite data used to generate the burned-area products.

B. Regional Product Accuracy and Precision

Figs. 5–7 show scatter plots of the proportion of area burned in 5×5 km grid cells, as defined by the three products (y -axis) and by the Landsat data (x -axis) for all the 11 validation sites. Because of the large number of cells considered, a grayscale shading scheme is used to illustrate the frequency of cells having the same x - and y -axis proportion values. A total of 11 747 cells, covering 294 851 km², are considered for the GlobCarbon and L3JRC products, and a slightly smaller number (11 719 cells), covering 294 148 km², are considered for the MODIS product because only MODIS cells with less than 10% missing MODIS pixels were considered. The coefficient of determination (r^2) and the equation of the estimated regression line are reported for each burned-area product.

The linear regression lines all pass close to the origin (absolute values of the regression line intercept less than 0.015) but with variable slopes from 0.136 (L3JRC), 0.595 (GlobCarbon), to 0.750 (MODIS). A slope of one indicates that the product estimates the same extent of area burned as the Landsat independent reference data, while a slope less

TABLE II
CONFUSION MATRIX VALIDATION RESULTS FOR THE
L3JRC BURNED AREA PRODUCT

Country Landsat Path/Row	Percentage Burned Landsat (%)	Percentage Burned L3JRC (%)	Percent Correct (%)	Comission Error (0-1)	Omision Error (0-1)
Mozambique 165/070	11.50	2.54	89.14	0.3735	0.8617
South Africa 168/078	3.63	1.40	96.26	0.5410	0.8230
South Africa 168/077	4.22	2.14	94.78	0.7355	0.8660
Malawi 169/069	3.26	0.17	96.70	0.6388	0.9815
Zimbabwe 169/074	7.04	2.82	91.55	0.7497	0.8996
Zimbabwe 171/073	5.62	1.67	94.98	0.3732	0.9862
Zimbabwe 172/073	5.05	0.11	94.98	0.3732	0.9862
Botswana 174/074	1.45	0.016	98.55	0.3366	0.9928
Botswana 175/073	7.76	0.08	92.19	0.7757	0.9976
	11.21	0.38	88.86	0.4138	0.9801
Namibia 179/073	1.83	0.03	98.15	1.0000	1.0000
Namibia 180/073	4.98	1.73	96.65	0.0263	0.6627

TABLE III
CONFUSION MATRIX VALIDATION RESULTS FOR THE
GlobCarbon BURNED AREA PRODUCT

Country Landsat Path/Row	Percentage Burned Landsat (%)	Percentage Burned Globcarbon (%)	Percent Correct (%)	Comission Error (0-1)	Omision Error (0-1)
Mozambique 165/070	11.50	3.78	88.73	0.4697	0.8259
South Africa 168/078	3.63	2.89	95.94	0.5739	0.6605
South Africa 168/077	4.22	4.72	95.96	0.4818	0.4192
Malawi 169/069	3.26	0.86	96.12	0.8630	0.9639
Zimbabwe 169/074	7.04	10.43	88.56	0.7109	0.5718
Zimbabwe 171/073	5.62	3.82	93.21	0.6524	0.7639
Zimbabwe 172/073	5.05	1.26	94.98	0.4883	0.8726
Botswana 174/074	1.45	1.16	99.04	0.2888	0.4293
Botswana 175/073	7.76	7.24	93.67	0.4012	0.4413
	11.21	8.10	89.73	0.4423	0.5965
Namibia 179/073	1.83	6.92	92.66	0.8985	0.6151
Namibia 180/073	4.98	5.84	96.60	0.3641	0.2547

than one indicates a burned-area underestimation, and a slope greater than one indicates an overestimation. Clearly, while all three global burned-area products underestimate the area burned at subcontinental scale, the L3JRC product particularly underestimates the area burned compared to the other two products. The near-zero intercepts and the slope values

TABLE IV
CONFUSION MATRIX VALIDATION RESULTS FOR THE
MODIS BURNED AREA PRODUCT

Country Landsat Path/Row	Percentage Burned Landsat (%)	Percentage Burned MODIS (%)	Percent Correct (%)	Comission Error (0-1)	Omision Error (0-1)
Mozambique 165/070	11.50	7.10	90.98	0.3250	0.5833
South Africa 168/078	3.63	1.75	96.14	0.5648	0.7906
South Africa 168/077	4.23	3.74	96.32	0.4274	0.4937
Malawi 169/069	3.26	0.54	96.57	0.6549	0.9428
Zimbabwe 169/074	7.04	4.57	92.66	0.5323	0.6966
Zimbabwe 171/073	5.62	2.84	95.56	0.2915	0.6426
Zimbabwe 172/073	5.05	2.26	96.63	0.1295	0.6102
Botswana 174/074	1.45	0.75	99.06	0.1577	0.5625
Botswana 175/073	7.76	5.97	97.20	0.0842	0.2955
	11.21	8.09			
Namibia 179/073	1.83	0.34	98.15	0.5462	0.9145
Namibia 180/073	4.98	5.19	99.32	0.0860	0.0470

indicate that at subcontinental scale, the MODIS, GlobCarbon, and L3JRC burned-area products can be expected to capture 75%, 60%, and 14% of the true area burned, respectively. It is not unexpected that the L3JRC product maps a smaller extent of area burned than GlobCarbon, as the GlobCarbon algorithm includes an independent implementation of the L3JRC algorithm and two other algorithms (Section II-B). We note that [66] reported a significantly higher L3JRC slope (0.54) than the 0.136 value that we observe. However, these two estimates are not directly comparable, as the analysis in [66] used grid cells that are two orders of magnitude greater (3000 km²) and because they considered a different year and included northern Africa where the fire behavior is considerably different than that in southern Africa [8].

The dispersion of the data around the regression line, quantified by the coefficient of determination (r^2), reflects the precision of the burned-area detection. A coefficient of determination equal to one indicates that the variability of the data is fully explained by the linear model (all the points fall on the regression line), while a coefficient of determination equal to zero indicates that there is no relationship between the linear model and the variability of the data. The coefficient of determination follows the same pattern as the slope of the regression line for the three burned-area products: L3JRC has the lowest r^2 (0.128) compared to GlobCarbon ($r^2 = 0.509$) and MODIS ($r^2 = 0.746$). This pattern is evident in the scatter of the data around the regression lines seen in Figs. 5–7.

The regional regression results shown in Figs. 5–7 were computed including 5×5 km grid cells that had no proportion burned in both the Landsat data and the burned-area product. Such grid cells contain useful information, i.e., that there was

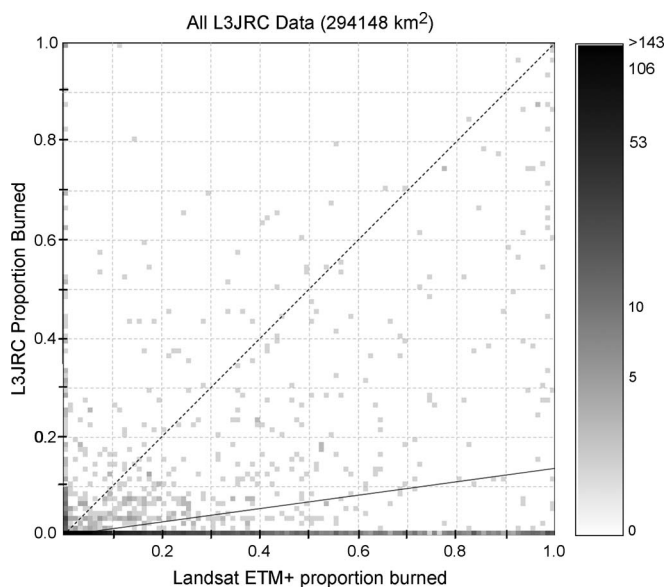


Fig. 5. Scatter plot of the proportions of 5×5 km cells labeled as burned by the L3JRC burned-area product plotted against the proportion labeled as burned by the multidecade Landsat interpretation. The grid lines show proportion intervals of 0.1. The regression line is plotted as a solid black line. The white-black logarithmic color scale represents the point density distribution of the scatter plot, using a 100×100 quantization of the x - and y -axes. Each point is plotted with a gray shade corresponding to the number of cells with the same (x, y) values. A total of 11 747 cells (total area of 294 851 km^2) are plotted. The slope of the regression line is 0.136, the intercept is 0.001, and the r^2 is 0.128.

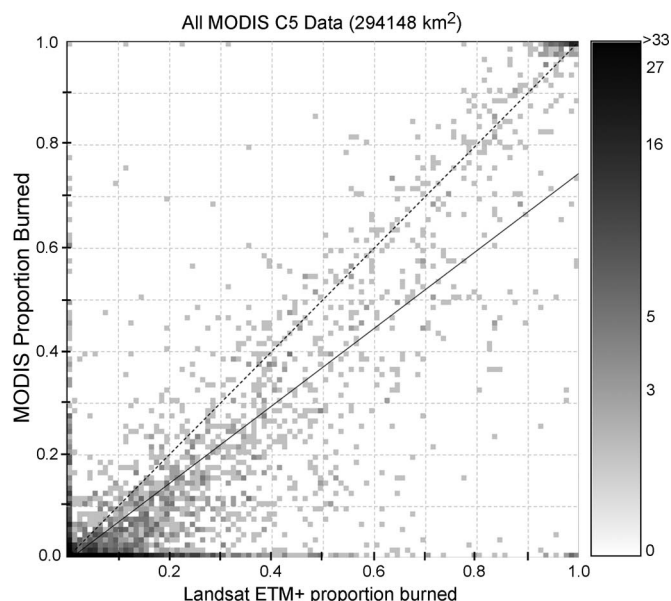


Fig. 7. Scatter plot of the proportions of 5×5 km cells labeled as burned by the MODIS burned-area product plotted against the proportion labeled as burned by the multidecade Landsat interpretation. Note that only 5×5 km cells with less than 10% of their area missing are considered; consequently, 11 719 cells (total area of 294 148 km^2), i.e., 29 fewer than the L3JRC and GlobCarbon products which had no missing class, are plotted. The slope of the regression line is 0.75, the intercept is -0.005 , and the r^2 is 0.746.

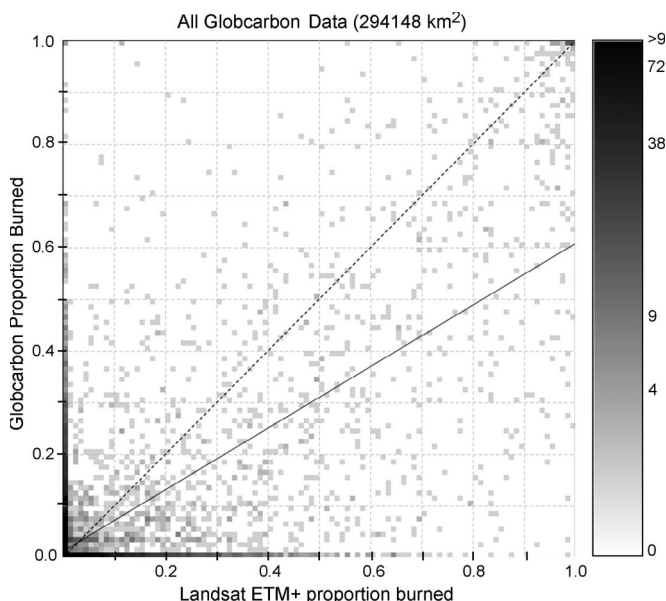


Fig. 6. Scatter plot of the proportions of 5×5 km cells labeled as burned by the GlobCarbon burned-area product plotted against the proportion labeled as burned by the multidecade Landsat interpretation. A total of 11 747 cells (total area of 294 851 km^2) are plotted. The slope of the regression line is 0.595, the intercept is 0.013, and the r^2 is 0.509.

no burning, which is not known *a priori*. Excluding them does not provide a true validation, but it is interesting to note the impact of their exclusion on the regression results: The r^2 is reduced for all products (0.090 for L3JRC, 0.447 for GlobCarbon, and 0.707 for MODIS); the intercepts change slightly (0.005 for L3JRC, 0.031 for GlobCarbon, and -0.018

for MODIS), and the slopes are reduced for L3JRC (0.129) and GlobCarbon (0.560) and increased slightly for MODIS (0.775). Thus, the impact of excluding grid cells with no proportion burned in either the Landsat or the burned-area product does not change the results; essentially, for regional applications, the more accurate and precise products in decreasing order are MODIS, then GlobCarbon, and then L3JRC.

VII. CONCLUSION

This paper presents a southern Africa validation of three available global multiannual burned-area products: L3JRC [66], GlobCarbon [44], and MODIS [50]. Independent reference data were located across southern Africa aimed at capturing a range of representative conditions and so providing a CEOS Stage 2 validation [38]. Based on independent reference data at 11 Landsat scenes, covering approximately 295 000 km^2 , the accuracy of the products was quantified using metrics derived from confusion matrices to characterize product accuracy for local applications and using metrics derived through a linear regression on a 5×5 km grid to characterize product accuracy for coarser scale applications.

All three products had generally lower errors of commission than omission. This is likely because burned-area product producers often seek to reduce errors of commission at a cost of inflating omission errors, as certain product users do not wish to waste resources on visiting burned areas that did not actually occur [68] and because commission errors are more easily identified as part of product quality assessment and algorithm tuning procedures. The actual errors of omission are probably higher than reported, as the independent reference data only included Landsat-mapped burned areas

with small axis dimensions of 240 m or greater. Our findings suggest the following: 1) product developers should attempt to more evenly balance omission and commission errors, and 2) global burned-area products may not meet the accuracy needs of local users, although these needs are diverse and the accuracy requirements are not well defined [68].

The MODIS product provided higher burned-area mapping accuracies than the other two products, which may be due to the higher 500-m MODIS spatial resolution, which improves the ability to detect small and spatially fragmented burned areas [49], to the comprehensive calibration, geolocation, cloud screening, and atmospheric correction of the MODIS land data [26], [27], [34] and perhaps to the specifics of the MODIS burned-area algorithm [50]. The GlobCarbon product provided higher burned-area mapping accuracies than the L3JRC product. This may be due to the treatment in this paper of GlobCarbon pixels as burned if any of the GlobCarbon algorithms, which included an independent implementation of the L3JRC algorithm, labeled pixels as burned and because the L3JRC product had relatively higher omission errors.

It is our intention to build on this paper, using the multirate high spatial resolution satellite data approach to validate, to CEOS Validation Stage 2, the MODIS burned-area product globally, with an emphasis on sampling in each continent a range of representative conditions and where the algorithm has known limitations [53]. It is possible to envision a CEOS Stage 3 validation where the independent reference data are obtained by a random sampling procedure in both space and time [38]. However, the nature of burned areas as a nonpermanent land-cover change [41], [67], coupled with the relative global scarcity of cloud-free high spatial resolution data [24], and the need for rigorous interpretation of such data, requires considerable resources that may only be available in the framework of an international validation effort.

These results reinforce the need for systematic burned-area product validation discussed in Section I. This need can be expected to increase as more satellite burned-area products become available, driven by factors including increasing computer processing and storage capabilities, space agency support for low-cost and free satellite data, and the proliferation of direct broadcast satellite reception systems.

REFERENCES

- [1] S. Archibald, D. P. Roy, B. W. Van Wilgen, and R. J. Scholes, "What limits fire?: An examination of drivers of burnt area in sub-equatorial Africa," *Glob. Chang. Biol.*, vol. 15, pp. 613–630, 2009. DOI: 10.1111/j.1365-2486.2008.01754.x.
- [2] T. Arvidson, J. Gasch, and S. N. Goward, "Landsat 7's long-term acquisition plan—An innovative approach to building a global imagery archive," *Remote Sens. Environ.*, vol. 78, no. 1, pp. 13–26, Oct. 2001.
- [3] P. M. Barbosa, D. Stroppiano, J. M. Grégoire, and J. M. C. Pereira, "An assessment of vegetation fire in Africa (1981–1991): Burned areas, burned biomass, and atmospheric emissions," *Glob. Biogeochem. Cycles*, vol. 13, no. 4, pp. 933–950, 1999.
- [4] W. J. Bond, F. I. Woodward, and G. F. Midgley, "The global distribution of ecosystems in a world without fire," *New Phytol.*, vol. 165, no. 2, pp. 525–538, Mar. 2005.
- [5] L. Boschetti, H. Eva, P. A. Brivio, and J. M. Grégoire, "Lessons to be learned from the comparison of three satellite-derived biomass burning products," *Geophys. Res. Lett.*, vol. 31, no. 21, pp. L21 501.1–L21 501.4, Nov. 2004. DOI: 10.1029/2004GL021229.
- [6] L. Boschetti, S. Flasse, and P. A. Brivio, "Analysis of the conflict between omission and commission in low spatial resolution dichotomic thematic products: The Pareto Boundary," *Remote Sens. Environ.*, vol. 91, no. 3/4, pp. 280–292, Jun. 2004.
- [7] L. Boschetti, P. A. Brivio, H. Eva, J. Gallego, A. Baraldi, and J. M. Grégoire, "A sampling method for the retrospective validation of global burned area products," *IEEE Trans. Geosci. Remote Sens.*, vol. 44, no. 7, pp. 1765–1773, Jul. 2006.
- [8] L. Boschetti and D. P. Roy, "Defining a fire year for reporting and analysis of global interannual fire variability," *J. Geophys. Res.*, vol. 113, no. G3, p. G03 020, Aug. 2008. DOI:10.1029/2008JG000686.
- [9] M. F. Cardoso, G. C. Hurtt, B. Moore, C. A. Nobre, and E. Prins, "Projecting future fire activity in Amazonia," *Glob. Change Biol.*, vol. 9, no. 5, pp. 656–669, May 2003.
- [10] R. G. Congalton, R. G. Oderwald, and R. A. Mead, "Assessing Landsat classification accuracy using discrete multivariate analysis statistical techniques," *Photogramm. Eng. Remote Sens.*, vol. 49, pp. 1671–1678, 1983.
- [11] I. Csizsar, J. T. Morisette, and L. Giglio, "Validation of active fire detection from moderate-resolution satellite sensors: The MODIS example in Northern Eurasia," *IEEE Trans. Geosci. Remote Sens.*, vol. 44, no. 7, pp. 1757–1764, Jul. 2006.
- [12] I. Csizsar, C. O. Justice, J. G. Goldammer *et al.*, "The GOCF–GOLD fire mapping and monitoring theme: Assessment and strategic plans," in *Earth Science Satellite Remote Sensing*. Dordrecht, The Netherlands: Springer-Verlag, to be published.
- [13] E. Dwyer, S. Pinnock, J.-M. Grégoire, and J. M. C. Pereira, "Global spatial and temporal distribution of vegetation fire as determined from satellite observations," *Int. J. Remote Sens.*, vol. 21, no. 6/7, pp. 1289–1302, Apr. 2000.
- [14] D. V. Ershov and V. P. Novik, "Mapping burned areas in Russia with SPOT4 VEGETATION (S1 product) imagery," Joint Res. Centre Eur. Comm., Ispra, Italy, 2001. Contract Number: 18176-2001-07-F1EI ISP RU.
- [15] H. Eva and E. F. Lambin, "Remote sensing of biomass burning in tropical regions: Sampling issues and multisensor approach," *Remote Sens. Environ.*, vol. 64, no. 3, pp. 292–315, Jun. 1998.
- [16] D. A. Falk, C. Miller, D. McKenzie, and A. E. Black, "Cross-scale analysis of fire regimes," *Ecosystems*, vol. 10, no. 5, pp. 809–823, Aug. 2007.
- [17] R. H. Fraser, Z. Li, and J. Cihlar, "Hotspot and NDVI differencing synergy (HANDS)—A new technique for burned area mapping over boreal forest," *Remote Sens. Environ.*, vol. 74, no. 3, pp. 362–376, Dec. 2000.
- [18] G. Foody, "Status of land cover classification accuracy assessment," *Remote Sens. Environ.*, vol. 80, no. 1, pp. 185–201, Apr. 1992.
- [19] P. G. H. Frost, "Fire in Southern African woodlands: Origins, impacts, effects, and control," in *Proc. FAO Meeting Public Policies Affecting Forest Fires*, 1999, pp. 181–205.
- [20] GCOS/GTOS, *The GCOS/GTOS Plan for Terrestrial Climate Related Observations*, 1997, Geneva, Switzerland. GCOS Document #32, WMO Tech. Doc. 796.
- [21] J.-M. Grégoire, K. Tansey, and J. M. N. Silva, "The GBA2000 initiative: Developing a global burnt area database from SPOT-VEGETATION imagery," *Int. J. Remote Sens.*, vol. 24, no. 6, pp. 1369–1376, Mar. 2003.
- [22] T. J. Hawbaker, V. C. Radeloff, A. D. Syphard, Z. Zhu, and S. I. Stewart, "Detection rates of the MODIS active fire product in the United States," *Remote Sens. Environ.*, vol. 112, no. 5, pp. 2656–2664, May 15, 2008.
- [23] G. J. Huffman, R. F. Adler, B. Rudolph, U. Schneider, and P. Keehn, "Global precipitation estimates based on a technique for combining satellite-based estimates, rain gauge analysis, and NWP model precipitation information," *J. Clim.*, vol. 8, no. 5, pp. 1284–1295, May 1995.
- [24] J. Ju and D. P. Roy, "The availability of cloud-free Landsat ETM+ data over the conterminous United States and globally," *Remote Sens. Environ.*, vol. 112, no. 3, pp. 1196–1211, Mar. 2008.
- [25] C. O. Justice, A. Belward, J. Morisette, P. Lewis, J. Privette, and F. Baret, "Developments in the 'validation' of satellite sensor products for the study of the land surface," *Int. J. Remote Sens.*, vol. 21, no. 17, pp. 3383–3390, Nov. 2000.
- [26] C. Justice, L. Giglio, S. Korontzi, J. Owens, J. Morisette, D. Roy, J. Descloitres, S. Alleaume, F. Peticoloin, and Y. Kaufman, "The MODIS fire products," *Remote Sens. Environ.*, vol. 83, no. 1/2, pp. 244–262, Nov. 2002.
- [27] C. Justice, J. Townshend, E. Vermote, E. Masuoka, R. Wolfe, N. Saleous, D. Roy, and J. Morisette, "An overview of MODIS Land data processing and product status," *Remote Sens. Environ.*, vol. 83, no. 1, pp. 3–15, Nov. 2002.
- [28] C. O. Justice, R. Smith, M. Gill, and I. Csizsar, "Satellite-based fire monitoring: Current capabilities and future directions," *Int. J. Wildland Fire*, vol. 12, no. 4, pp. 247–258, 2003.

- [29] Y. J. Kaufman, C. O. Justice, L. P. Flynn, J. D. Kendall, E. M. Prins, L. Giglio, D. E. Ward, P. Menzel, and A. Setzer, "Potential global fire monitoring from EOS-MODIS," *J. Geophys. Res.*, vol. 103, no. D24, pp. 32 215–32 238, 1998.
- [30] S. Korontzi, D. P. Roy, C. O. Justice, and D. E. Ward, "Modeling and sensitivity analysis of fire emissions in Southern Africa during SAFARI 2000," *Remote Sens. Environ.*, vol. 92, no. 2, pp. 255–275, Aug. 2004.
- [31] P. Laris, "Spatiotemporal problems with detecting and mapping mosaic fire regimes with coarse-resolution satellite data in savanna environments," *Remote Sens. Environ.*, vol. 99, no. 4, pp. 412–424, Dec. 2005.
- [32] D. S. Lee, J. C. Storey, M. J. Choate, and R. Hayes, "Four years of Landsat-7 on-orbit geometric calibration and performance," *IEEE Trans. Geosci. Remote Sens.*, vol. 42, no. 12, pp. 2786–2795, Dec. 2004.
- [33] R. Leemans and W. P. Kramer, "The IIASA database for mean monthly values of temperature, precipitation and cloudiness of a global terrestrial grid," *Int. Inst. Appl. Syst. Anal.*, Laxenburg, Austria, p. 60, IIASA Res. Rep. RR-91-18, 1990.
- [34] E. Masuoka, D. P. Roy, R. Wolfe, J. Morisette, M. Teague, N. Saleous, S. Devadiga, C. Justice, S. Sinno, and J. Nickeson, "MODIS land data products: Generation, quality assurance and validation," in *Land Remote Sensing and Global Environmental Change: NASA's EOS and the Science of ASTER and MODIS*, B. Ramachandran, C. Justice, and M. Abrams, Eds. New York: Springer-Verlag, 2008.
- [35] P. Mayaux, E. Bartholomé, S. Fritz, and A. Belward, "A new land-cover map of Africa for the year 2000," *J. Biogeogr.*, vol. 31, no. 6, pp. 861–877, Jun. 2004.
- [36] J. T. Morisette, J. L. Privette, and C. O. Justice, "A framework for the validation of MODIS Land products," *Remote Sens. Environ.*, vol. 83, no. 1, pp. 77–96, Nov. 2002.
- [37] J. Morisette, L. Giglio, I. Csiszar, and C. Justice, "Validation of the MODIS active fire product over southern Africa with ASTER data," *Int. J. Remote Sens.*, vol. 26, no. 19, pp. 4239–4264, Oct. 2005.
- [38] J. T. Morisette, F. Baret, and S. Liang, "Special issue on global land product validation," *IEEE Trans. Geosci. Remote Sens.*, vol. 44, no. 7, pp. 1695–1697, Jul. 2006.
- [39] S. Openshaw, "The modifiable areal unit problem," in *Concepts and Techniques in Modern Geography*. Norwich, U.K.: Geo Books, 1984.
- [40] I. Piccolini, "Development and validation of an adaptive algorithm for burn scar detection using ERS/ATSR-2 data," Ph.D. dissertation, Univ. la Sapienza, Rome, Italy, 1998.
- [41] J. M. C. Pereira, E. Chuvieco, A. Beaudoin, and N. Desbois, "Remote sensing of burned areas," in *A Review of Remote Sensing Methods for the Study of Large Wildland Fires*, E. Chuvieco, Ed. Alcalá de Henares, Spain: Univ. de Alcalá, Aug. 1997, pp. 127–183.
- [42] J. M. C. Pereira, M. Bernardo, J. L. Privette, K. K. Caylor, J. M. N. Silva, A. C. L. Sá, and N.-M. Wenge, "A simulation analysis of the detectability of understory burns in Miombo woodlands," *Remote Sens. Environ.*, vol. 93, no. 3, pp. 296–310, Nov. 2004.
- [43] A. C. Pereira and A. W. Setzer, "Comparison of fire detection in savannas using AVHRR's channel 3 and TM images," *Int. J. Remote Sens.*, vol. 17, no. 10, pp. 1925–1937, Jul. 1996.
- [44] S. Plummer, O. Arino, M. Simon, and W. Steffen, "Establishing a Earth observation product service for the terrestrial carbon community: The GlobCarbon initiative," *Mitig. Adapt. Strategies Glob. Chang.*, vol. 11, no. 1, pp. 97–111, Jan. 2006.
- [45] J. L. Privette and D. P. Roy, "Southern Africa as a remote sensing test bed: The SAFARI 2000 Special Issue overview," *Int. J. Remote Sens.*, vol. 26, no. 19, pp. 4141–4158, Oct. 2005.
- [46] K. Rasmussen, J. Russell-Smith, J. T. Morisette, *Establishing a validation site network for remote sensing applications to fire research: A joint activity between GOCF-Fire and the LPV subgroup*, 2001. White paper. [Online]. Available: http://modis.gsfc.nasa.gov/MODIS/LAND/VAL/CEOS_WGCV/GOCF_LPV_fire_sites.pdf
- [47] D. P. Roy and O. Dikshit, "Investigation of image resampling effects upon the textural information content of a high spatial resolution remotely sensed image," *Int. J. Remote Sens.*, vol. 15, no. 5, pp. 1123–1130, Mar. 1994.
- [48] D. P. Roy, J. Borak, S. Devadiga, R. Wolfe, M. Zheng, and J. Desclotres, "The MODIS land product quality assessment approach," *Remote Sens. Environ.*, vol. 83, no. 1, pp. 62–76, Nov. 2002.
- [49] D. P. Roy and T. Landmann, "Characterizing the surface heterogeneity of fire effects using multi-temporal reflective wavelength data," *Int. J. Remote Sens.*, vol. 26, no. 19, pp. 4197–4218, Oct. 2005.
- [50] D. P. Roy, Y. Jin, P. E. Lewis, and C. O. Justice, "Prototyping a global algorithm for systematic fire-affected area mapping using MODIS time series data," *Remote Sens. Environ.*, vol. 97, no. 2, pp. 137–162, Jul. 2005.
- [51] D. P. Roy, P. Frost, C. Justice, T. Landmann, J. Le Roux, K. Gumbo, S. Makungwa, K. Dunham, R. Du Toit, K. Mhwandagara, A. Zacarias, B. Tacheba, O. Dube, J. Pereira, P. Mushove, J. Morisette, S. Santhana Vannan, and D. Davies, "The Southern Africa Fire Network (SAFNet) regional burned-area product-validation protocol," *Int. J. Remote Sens.*, vol. 26, no. 19, pp. 4265–4292, Oct. 2005.
- [52] D. P. Roy, S. N. Trigg, R. Bhima, B. Brockett, O. Dube, P. Frost, N. Govender, T. Landmann, J. Le Roux, T. Lepono, J. Macuacua, C. Mbow, K. Mhwandagara, B. Mosepele, O. Mutanga, G. Neo-Mahupeleng, M. Norman, and S. Virgilo, "The utility of satellite fire product accuracy information—Perspectives and recommendations from the Southern Africa fire network," *IEEE Trans. Geosci. Remote Sens.*, vol. 44, no. 7, pp. 1928–1930, Jul. 2006.
- [53] D. P. Roy, L. Boschetti, C. O. Justice, and J. Ju, "The Collection 5 MODIS burned area product—Global evaluation by comparison with the MODIS active fire product," *Remote Sens. Environ.*, vol. 112, no. 9, pp. 3690–3707, Sep. 2008.
- [54] D. P. Roy, J. Ju, P. Lewis, C. Schaaf, F. Gao, M. Hansen, and E. Lindquist, "Multi-temporal MODIS-Landsat data fusion for relative radiometric normalization, gap filling, and prediction of Landsat data," *Remote Sens. Environ.*, vol. 112, no. 6, pp. 3112–3130, Jun. 2008.
- [55] R. J. Scholes, "Savanna," in *Vegetation of Southern Africa*, R. M. Cowling, D. M. Richardson, and S. M. Pierce, Eds. Cambridge, U.K.: Cambridge Univ. Press, 1997, pp. 258–277.
- [56] R. J. Scholes, P. R. Dowty, K. Caylor, D. A. B. Parsons, P. G. H. Frost, and H. H. Shugart, "Trends in savanna structure and composition along an aridity gradient in the Kalahari," *J. Veg. Sci.*, vol. 13, no. 3, pp. 419–428, Jun. 2002.
- [57] M. Simon, S. Plummer, F. Fierens, J. J. Hoeltzemann, and O. Arino, "Burnt area detection at global scale using ATSR-2: The GLOBSCAR products and their qualification," *J. Geophys. Res.*, vol. 109, no. D14, p. D14 S02, Jul. 2004. DOI: 10.1029/2003JD003622.
- [58] J. M. N. Silva, J. M. C. Pereira, A. I. Cabral, A. C. L. Sá, P. Vasconcelos, B. Mota, and J.-M. Grégoire, "An estimate of the area burned in southern Africa during the 2000 dry season using SPOT-VEGETATION satellite data," *J. Geophys. Res.*, vol. 108, no. D13, p. 8498, Apr. 2003. DOI: 10.1029/2002JD002320.
- [59] J. M. N. Silva, A. C. L. Sá, and J. M. C. Pereira, "Comparison of burned area estimates derived from SPOT-VEGETATION and Landsat ETM+ data in Africa: Influence of spatial pattern and vegetation type," *Remote Sens. Environ.*, vol. 96, no. 2, pp. 188–201, May 2005.
- [60] A. M. S. Smith, N. A. Drake, M. J. Wooster, A. T. Hudak, Z. A. Holden, and C. J. Gibbons, "Production of Landsat ETM+ reference imagery of burned areas within Southern African savannahs: Comparison of methods and application to MODIS," *Int. J. Remote Sens.*, vol. 28, no. 12, pp. 2753–2775, 2007.
- [61] A. Strahler, L. Boschetti, G. Foody, M. Friedl, M. Hansen, M. Harold, P. Mayaux, J. Morisette, S. Stehman, and C. Wodcock, "Global land cover validation: Recommendations for evaluation and accuracy assessment of global land cover maps," Office Official Publ. Eur. Commun., Luxembourg, Belgium, p. 58, EUR 22156 EN, 2006.
- [62] R. Stöckli, E. Vermote, N. Saleous, R. Simmon, and D. Herring, "True color earth data set includes seasonal dynamics," *EOS, Trans. Amer. Geophys. Union*, vol. 87, no. 5, pp. 49–55, Jan. 2006.
- [63] M. Story and R. G. Congalton, "Accuracy assessment: A user's perspective," *Photogramm. Eng. Remote Sens.*, vol. 52, no. 3, pp. 397–399, 1986.
- [64] R. J. Swap, H. J. Annegarn, J. T. Suttles, J. Haywood, M. C. Helmlinger, C. Hely, P. V. Hobbs, B. N. Holben, J. Ji, M. King, T. Landmann, W. Maenhaut, L. Otter, B. Pak, S. J. Piketh, S. Platnick, J. Privette, D. P. Roy, A. M. Thompson, D. Ward, and R. Yokelson, "The Southern African regional science initiative (SAFARI 2000): Overview of the dry-season field campaign," *South African J. Sci.*, vol. 98, no. 3/4, pp. 125–130, 2002.
- [65] K. Tansey, J.-M. Grégoire, D. Stroppiana, A. Sousa, J. M. N. Silva, J. M. C. Pereira, L. Boschetti, M. Maggi, P. A. Brivio, R. Fraser, S. Flasse, D. Ershov, E. Binaghi, D. Graetz, and P. Peduzzi, "Vegetation burning in the year 2000: Global burned area estimates from SPOT VEGETATION data," *J. Geophys. Res.*, vol. 109, no. D14, p. D14 S03, Jun. 2004. DOI:10.1029/2003JD003598.
- [66] K. Tansey, J. M. C. Grégoire, P. Defourny, R. Leigh, J.-F. Pekel, E. van Bogaert, E. Bartholomé, and S. Bontemps, "A new, global, multi-annual (2000–2007) burned area product at 1 km resolution and daily intervals," *Geophys. Res. Lett.*, vol. 35, no. 1, p. L01401, 2008. DOI:10.1029/2007GL031567.
- [67] S. Trigg and S. Flasse, "Characterizing the spectral-temporal response of burned savannah using *in situ* spectroradiometry and infrared thermometry," *Int. J. Remote Sens.*, vol. 21, no. 16, pp. 3161–3168, Nov. 2000.

- [68] S. N. Trigg and D. P. Roy, "A focus group study of factors that promote and constrain the use of satellite derived fire products by resource managers in Southern Africa," *J. Environ. Manag.*, vol. 82, no. 1, pp. 95–110, 2007.
- [69] D. J. Unwin, "GIS, spatial analysis and spatial statistics," *Prog. Hum. Geogr.*, vol. 20, no. 4, pp. 540–541, 1996.
- [70] B. W. Van Wilgen and R. J. Scholes, "The vegetation and fire regimes of southern hemisphere Africa," in *Fire in Southern African Savannas: Ecological and Atmospheric Perspectives*, M. O. Andreae, J. G. Goldammer, and K. Lindsay, Eds. Johannesburg, Africa: Witwatersrand Univ. Press, 1997, pp. 27–46.
- [71] G. F. Van Der Werf, T. Randerson, L. Giglio, G. J. Collatz, P. S. Kasibhatla, and A. F. Arellano, "Interannual variability in global biomass burning emissions from 1997 to 2004," *Atmos. Chem. Phys.*, vol. 6, no. 11, pp. 3423–3441, Aug. 2006.
- [72] R. Wolfe, D. Roy, and E. Vermote, "MODIS land data storage, gridding, and compositing methodology: Level 2 grid," *IEEE Trans. Geosci. Remote Sens.*, vol. 36, no. 4, pp. 1324–1338, Jul. 1998.
- [73] R. Wolfe, M. Nishihama, A. Fleig, J. Kuyper, D. Roy, J. Storey, and F. Patt, "Achieving sub-pixel geolocation accuracy in support of MODIS land science," *Remote Sens. Environ.*, vol. 83, no. 1, pp. 31–49, Nov. 2002.
- [74] *CEOS Response to the GCOS Implementation Plan, Satellite Observation of the Climate System*, last accessed June 9th 2008, WWW1. [Online]. Available: <http://www.ceos.org/CEOS%20Response%20to%20the%20GCOS%20IP.pdf>
- [75] WWW2. last accessed June 9th 2008. [Online]. Available: <http://www.GlobCarbon.info>
- [76] WWW3. last accessed June 9th 2008. [Online]. Available: <http://www.spot-vegetation.com>



David P. Roy received the B.Sc. degree in geophysics from the University of Lancaster, Lancaster, U.K., in 1987, the M.Sc. degree in remote sensing and image processing technology from the University of Edinburgh, Edinburgh, U.K., in 1988, and the Ph.D. degree in remote sensing from the University of Cambridge, Cambridge, U.K., in 1994.

He was a Research Fellow with the National Environment Research Council for Thematic Information Systems, University of Reading, Reading, U.K., from 1993 to 1994 and with the Space Applications

Institute, Joint Research Centre, European Commission, Ispra, Italy, from 1994 to 1996. He was a Research Scientist with the Department of Geography, University of Maryland, College Park, and led the Moderate Resolution Imaging Spectroradiometer Land Data Operational Product Evaluation Group, Goddard Space Flight Center, NASA, for eight years. He has been with South Dakota State University, Brookings, since 2005, where he is currently a Professor with the Geographic Information Science Center of Excellence. His research interests include the development of remote sensing and advanced computing methods to map and characterize terrestrial change, in particular the occurrence and characteristics of vegetation fires, and land-cover–land-use–climate interactions.



Luigi Boschetti received the Laurea (M.S.) degree in environmental engineering and the Ph.D. degree in geodesy and geomatics from the Politecnico di Milano, Milano, Italy, in 2000 and 2005, respectively.

He was a Visiting Scientist with the Natural Resources Institute, University of Greenwich, London, U.K., from 2000 to 2002, a Research Fellow with the Institute for Environment and Sustainability, Joint Research Centre, European Commission, Ispra, Italy, from 2002 to 2004, and a Research Fellow with CNR—IREA, Milano, Italy, from 2004 to 2005. Since 2005, he has been a Research Scientist with the Department of Geography, University of Maryland, College Park. His research primarily includes the application of medium-resolution satellite data for environmental monitoring, with a focus on burned-area mapping, and the development of validation techniques for global thematic products.